PCCP

PAPER

View Article Online
View Journal | View Issue

Cite this: *Phys. Chem. Chem. Phys.*, 2021, **23**, 7974

CO_2 conversion by plasma: how to get efficient CO_2 conversion and high energy efficiency

Yongxiang Yin,*[a] Tao Yang,[ab] Zhikai Li,[a] Edwin Devid,[cd] Daniel Auerbach[ce] and Aart W. Kleyn*[c]

Received 7th October 2020,
Accepted 11th January 2021

DOI: 10.1039/d0cp05275b

rsc.li/pccp

Conversion of CO_2 into CO with plasma processing is a potential method to transform intermittent sustainable electricity into storable chemical energy. The main challenges for developing this technology are how to get efficient CO_2 conversion with high energy efficiency and how to prove its feasibility on an industrial scale. In this paper we review the mechanisms and performance of different plasma methodologies used in CO_2 conversion. Mindful of the goals of obtaining efficient conversion and high energy efficiency, as well as industrial feasibility in mind, we emphasize a promising new approach of CO_2 conversion by using a thermal plasma in combination with a carbon co-reactant.

1. Introduction

Atomic and molecular physics and surface science are enabling sciences. Better understanding of these fields of science will ultimately contribute to technological innovation, a cleaner environment, green energy, and more well-being for humankind. Peter Toennies has made strong contributions to these enabling sciences. He fully explained many elementary processes with atomistic rigor; furthermore, he obtained excellent agreement between experimental results and basic theory. It is interesting to explore to what extent these enabling sciences have enabled technological innovation.

In this paper, we review the development of plasma technology to convert the greenhouse gas CO_2 into more useful chemical compounds. In this endeavor, we will see many concepts and experimental methods in use that were developed in atomic and molecular physics. Towards the end of this article we also show that adding surface reactions to plasma technology provides a step forward to efficient conversion of greenhouse gasses using intermittent, sustainably generated electrical power. This work has benefited greatly from the enabling sciences, to which Peter Toennies has contributed so much.

Renewable energy sources, such as solar and wind, are expected to contribute significantly to the energy supply in the future; because of the intermittent nature of these energy sources, energy storage technologies are required.[1–6] In addition, concerns about the rising level of the CO_2 concentration in the atmosphere require that CO_2 generated by electrical power generation should not be released into the atmosphere and instead be converted into useful chemicals.[7–9] To maximize the reduction in CO_2 emission, clearly we must use renewable energy sources to carry out this conversion. By using renewable energy sources to convert CO_2 to chemical energy we overcome the problem that the production of renewable energy, usually harvested as electrical energy, is intermittent in daily-seasonal-regional variations and not matched in time with the energy demands of society. In addition, conversion of renewable energy to chemical energy can provide raw materials for the chemical industry. Therefore, effective storage and conversion of renewable electricity must be realized, and this must be done on an enormous scale.[1–3,9]

The time scale for energy storage can be short-term or long-term. Short-term storage, for hours, days or weeks, can be achieved through battery storage or pumped-storage.[10,11] However, long-term storage for seasons or years, is also required to ensure a stable energy supply and strategic security over several seasons. This kind of storage is not only required for a long time, but also involves a huge scale of energy storage: hundreds of terawatt hours (TWhs). It is hard to imagine any energy storage medium other than energetic chemicals like liquid and gaseous fuels that could meet such requirements. Both by volume and by weight hydrocarbon fuels are superior to other forms of energy storage.[8,9]

These considerations have motivated a truly massive effort over the last decade to develop methods to convert electricity produced in a renewable fashion into energetic chemicals.[1,3,9] One of these approaches is to use renewable electricity to

[a] *School of Chemical Engineering, Sichuan University, Chengdu 610065, Sichuan, China. E-mail: hyyx0675@sina.com*
[b] *School of Biological and Chemical Engineering, Panzhihua University, China*
[c] *Center of Interface Dynamics for Sustainability, Institute of Materials, China Academy of Engineering Physics, Chengdu 610200, Sichuan, China. E-mail: a.w.kleijn@contact.uva.nl*
[d] *DIFFER - Dutch Institute for Fundamental Energy Research, De Zaale 20, Eindhoven 5612 AJ, The Netherlands*
[e] *Max Planck Institute for Biophysical Chemistry, Göttingen, Germany*

convert CO_2 into CO, and subsequently into methane, methanol or liquid hydrocarbons using hydrogen from water electrolysis.[12–16] This approach not only enables conversion of renewable energy into chemical energy that can be easily stored, transported and distributed with existing infrastructure, but also offers a way to reduce carbon emissions.

One of the major challenges to doing this is achieving efficient conversion of CO_2 to CO using economical technologies that are viable on an industrial scale. This challenge has motivated explorations of conversion by a wide variety of methods.[17–21] Although each of these methods has its unique advantages and has achieved progress, in this review, we limit our attention to the discussion of CO_2 conversion using plasma technologies.[20–24] Besides direct conversion of pure CO_2 also mixtures of gasses such as CO_2 + CH_4 or CO_2 + H_2 can be converted to syngas (a mixture of CO + H_2), hydrocarbons and other compounds. Entries to the literature can be found in.[20,23,25,26]

The paper is arranged as follows. In Section 2, the features of different types of plasmas and the mechanisms of CO_2 splitting by plasma are briefly introduced. In Section 3, CO_2 conversion by non-thermal plasma is introduced. In Section 4, CO_2 conversion by thermal plasma is reviewed. It is shown that the conversion is limited by back-reactions, turning the products back into the reactant CO_2. In Section 5 it is shown that by chemical quenching using solid carbon the back-reaction can be suppressed. In this way high conversion, high energy efficiency and large power handling capacity can be realized. This can be done by reacting the plasma on a carbon surface, using the Boudouard reaction.[27]

2. Principle of CO_2 conversion by a plasma

Because plasmas are somewhat outside the scope of this issue, we will give a brief introduction. Additional introductory material on plasma chemistry can be found in recent text books.[28,29] A plasma is a partly ionized gas with its volume mean ionization degree (*i.e.*, ratio between density of major charged species to that of neutral gas) usually in the range 10^{-7} to 10^{-4}.[29] The simplest way to generate a plasma in the laboratory is to insert two metal electrodes connected to a power supply into a container with gas flow. When the voltage applied between the two electrodes is high enough, the gas between electrodes will be partly ionized by electron avalanches to form a plasma. An electron avalanche is initiated by a local ionization event, for instance by a cosmic ray. The electrons and ions in the plasma then continually get energy by acceleration in the electric field and transfer their kinetic energy to gas atoms or molecules (heavy neutral particles in general) by electronically elastic, otherwise inelastic collisions (inelastic in terms of momentum transfer). Neutral particles are activated by inelastic collisions with electrons in the plasma, resulting in electronic excitation and vibrational excitation, which can lead to decomposition and ionization. The latter step will maintain the plasma. Collisions can also transfer energy to the neutral particles which will heat them up.

Importantly, these excitation steps can stimulate chemical reactions that are impossible in conventional chemistry. For example, even chemically very stable CO_2 can be easily decomposed into CO, O, O_2 in plasma, and that is so-called CO_2 splitting by plasma. Simply speaking, a plasma is a system with charged particles and neutral particles, and it can easily convert electrical energy to molecular energy which in turn can activate chemical reactions.

2.1. Basic characteristics of plasmas used in CO_2 conversion

One of the notable features of plasma is that they often exhibit different temperatures for the different species and degrees of freedom in the system such as for electrons and neutral particles. The differences occur although the species are together in the same container. A rough estimation helps to understand the existence of temperature differences in plasma.

Electrons receive energy $\Delta\varepsilon_e$ from the electric field along their mean free path,

$$\Delta\varepsilon_e \approx \frac{1}{2m_e}\left(\frac{eEl}{u_e}\right)^2 \quad (1)$$

where $e = 1.602 \times 10^{-19}$ C, is the elementary charge, m_e is the mass of electron, l is the mean free path, u_e is the electron thermal velocity and E is the electric field strength in the plasma. At the same time, electrons transfer their energy to neutral particles by elastic collision. In each elastic collision, the energy transferred to neutral particle is $\delta\varepsilon_e$,

$$\delta\varepsilon_e \approx \frac{2m_e}{M}\frac{3}{2}k_b(T_e - T_g) \quad (2)$$

where M is the neutral particle mass, k_b the Boltzmann constant, T_e and T_g are the temperatures of the electrons and the neutral gas, respectively. Because an electron is much lighter than a heavy particle, the energy transferred from electron to neutral particle in each elastic collision is only a very small part of electron's energy. This allows the electron energy (or temperature) to grow gradually until the energy gained from the electric field is balanced with the energy transferred to the neutral particle, $\Delta\varepsilon_e = \delta\varepsilon_e$.

$$\frac{1}{2m_e}\left(\frac{eEl}{u_e}\right)^2 = \frac{2m_e}{M}\frac{3}{2}k_b(T_e - T_g). \quad (3)$$

The energy transfer from electrons to heavy particles by collision here is called ''Joule heating'' in an ionized gas. Obviously, the heating rate, $R_{heating}$, is proportional to electron density, n_e, and the elastic collision frequency, ν_e,

$$R_{heating} \approx n_e\nu_e\frac{2m_e}{M}\frac{3}{2}k_b(T_e - T_g) = \frac{n_e\nu_e}{2m_e}\left(\frac{eEl}{u_e}\right)^2 \quad (3^*)$$

Defining

$$\sigma = \frac{n_e e^2}{2m_e\nu_e}, \quad (4)$$

The ''Joule heating'' rate can be written in a familiar form, $R_{\text{heating}} = \sigma E^2$.

The heavy particles received energy from Joule heating and then their energy is transferred to the particles surrounding by thermal transmission, and finally reach at a steady state temperature, which can be simply determined by equation of heat conduction,

$$\nabla \cdot \kappa \nabla T_g = \sigma E^2 \tag{5}$$

where, ∇ is the gradient operator, $\nabla\cdot$ is the divergence operator, and κ is the heat conduction coefficient.

Theoretically, T_e and T_g can be determined by eqn (3) and (5), but it is difficult to do it because it involves many factors such as heat conduction and particle diffusion. However, when plasma system is in steady state, one can simply get the ratio of the electron temperature and heavy particle temperature with eqn (3).

Considering $l \approx (\sigma_{en} n_g)^{-1}$, $n_g = P/(k_b T_g)$, σ_{en}, the cross section of elastic collision, n_g, the density of heavy particles, P, the pressure in the plasma. We arrive at eqn (6),

$$\frac{T_e}{T_g} \approx \frac{1}{4}\left(\frac{M}{m_e}\right)^{\frac{1}{2}} \frac{e}{\sigma_{en}} \frac{E}{P} + 1 \approx 10^2 \frac{E}{P} + 1. \tag{6}$$

Obviously, in a model involving electronically elastic collisions, the ratio of the electron temperature and heavy particle temperature is only a function of (E/P).

In CO_2 gas discharges, $\frac{M}{m_e} \approx 7.3 \times 10^4$, $\sigma_{en} \approx 10^{-19}$ m^2, and the value of E/P is closely dependent on electron density, n_e. The higher the electron density in plasma, the lower the E/P value is. The typical features of three kinds of plasma frequently used in CO_2 conversion are listed in Table 1. For convenience, cold plasma and warm plasma are also jointly called non-thermal plasma to distinguish them from thermal plasma. The CO_2 conversion involved in these plasmas and the generation of the plasma will be discussed in detail in Sections 3 and 4.

2.2. Mechanisms of CO_2 conversion in plasma

The process of carbon dioxide conversion in a plasma starts with CO_2 splitting,

$$CO_2 \rightarrow CO + O,\ \Delta H = 5.5\ \text{eV}, \tag{7}$$

and reaches a stable situation by O-atom recombination into O_2 or an O-atom reaction with a co-reactant (if any) to create stable molecules. There are three main channels enabling in CO_2 splitting in a plasma, which are described in the following three sections.[28]

2.2.1. CO_2 splitting by direct electronic excitation

$$e + CO_2 \rightarrow e + CO_2^*(^1\Sigma_u^+) \rightarrow e + CO(^1\Sigma^+) + O(^1S) \tag{8}$$

This process is achieved by a single impact of an energetic electron with a CO_2 molecule. In the collision, the CO_2 molecule is excited from the ground state to an excited electronic state with an energy exceeding the dissociation enthalpy (5.5 eV). The molecule de-excites by energy transfer to O$\overline{\text{C}}$=O resulting in bond breaking. As the lowest electronic level of CO_2 is excited by more than 7 eV in the Franck–Condon region, the splitting of CO_2 molecules by electronic excitation is not very efficient. On one hand, the excess energy is taken away by translational energy transfer to the excited oxygen atom; on the other hand, the amount of electrons with sufficient excitation energy is limited as these energies are in the high energy tail of the electron energy distribution. The direct electronic excitation process mainly happens in a cold plasma with particularly high values of E/P, such as a plasma produced in a dielectric barrier discharge (DBD, where the electron density is low but the average electron energy is high).

2.2.2. CO_2 splitting by vibrational excitation,

$$\begin{aligned} &e + CO_2 \rightarrow e + CO_2^*(\nu_i) \\ &e + CO_2 \rightarrow e + CO_2^*(\nu_j) \\ &CO_2^*(\nu_i) + CO_2^*(\nu_j) \rightarrow CO_2^*(^3B_2) + CO_2 \\ &CO_2^*(^3B_2) \rightarrow CO(^1\Sigma^+) + O(^3P) \end{aligned} \tag{9}$$

This process involves a step-by-step vibrational excitation. The CO_2 molecules in the vibrational ground state are first excited to lower vibrational levels by electron impact; the vibrationally excited molecules transfer their vibrational energy among themselves in a vibrational–vibrational (V–V) relaxation process. Theoretically, some of them have a chance to be pumped up to a higher vibration energy level at the expense of vibrational de-excitation for other molecules. When the vibrational excitation reaches the dissociation threshold (5.5 eV), the CO_2 molecule can dissociate into CO and O in

Table 1 Typical features of three kinds of plasma used in CO_2 conversion

	n_e (cm^{-3})	E/P (V/P$_a$m)	T_e[a] (eV)	T_g (K)	P (Pa)	Discharge type[b]
Cold plasma	$\leq 10^{11}$	~ 0.1	~ 2	~ 300	≤ 100	GD
				~ 400 after 2 return and approximately 5 (see manuscript)	$\sim 10^5$	DBD
Warm plasma	10^{11}–10^{12}	~ 0.01	1–2	~ 1500–3000	$\sim 10^5$	GA
					10^3–10^4	MW or RF
Thermal plasma	$\geq 10^{13}$	~ 0.001	1–2	≥ 4000	$\sim 10^5$	ARC
						MW or RF

Table data compiled from ref. 28. [a] 1 eV = 11 605 K. [b] GD: glow discharge; DBD: dielectric barrier discharge; GA: gliding arc; MW: microwave discharge; RF: radio frequency discharge; ARC: alternating-current or direct-current arc discharge.

their ground state. This process is energy efficient for carbon dioxide splitting. However, there are two necessary conditions for significant V–V transfer to be satisfied. One is the electron temperature, T_e, of plasma should be about 1 eV in order to generate enough vibrational dynamic CO_2 molecules by numerous collisions of CO_2 with electrons; another is the translational temperature of the gas, T_g, must be less than the vibrational temperature to avoid vibrational-translational relaxation, causing depopulation of the CO_2 vibrational levels, as well gas heating, thus reducing the vibrational temperature and increasing the translational temperature.

2.2.3. CO_2 splitting by pyrolysis at high plasma temperature

$$CO_2 + M \rightarrow CO + O + M \quad E_a = 5.5 \text{ eV per molecule} \tag{10}$$

According to eqn (7), CO_2 splitting is a highly endothermic chemical reaction which is favored by high temperature. As shown in Fig. 1, from 2000 K upward, CO_2 conversion starts and the degree of dissociation increases with temperature, and the conversion rate of CO_2 can reach 75% at an equilibrium temperature of 3400 K. The pyrolysis products are CO, O and O_2 in the whole temperature range up to 4500 K. There is almost no C generated, implying that the selectivity of CO in thermal pyrolysis is 100%. Only at even higher temperatures CO is pyrolyzed as well.[28]

A thermal plasma driven by an arc discharge or microwave (MW) and radiofrequency (RF) discharge at atmospheric pressure can easily meet the conditions for CO_2 splitting. With the highest electron density among plasmas listed in Table 1, the gas temperature in this thermal plasma can be easily maintained at more than 4500 K by collisions. This makes CO_2 splitting possible not only by electronic excitation and vibrational excitation but also by pyrolysis.[20,28] However, the key problem in this pathway is how to avoid the reverse reactions, when the reaction products leave the high-temperature region of the plasma reactor. This will be discussed in the following paragraphs.

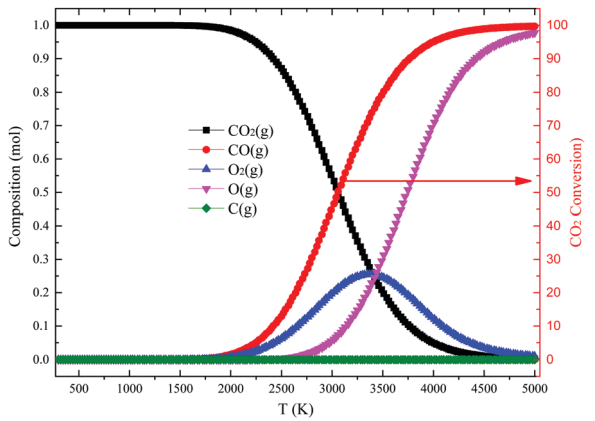

Fig. 1 Equilibrium composition (left) of CO_2 pyrolysis and CO_2 conversion (%, right) calculated by thermodynamics under normal pressure. see also ref. 28.

The three mechanisms of CO_2 splitting in a plasma described above reveal that the electron density in a plasma chemical process play a key role. This is a significant characteristic that allows plasma chemistry to differ from traditional chemistry. In cold plasma and warm plasma, CO_2 splitting is realized by electronic excitation or vibrational excitation, both are directly dependent on electron collisions. In a thermal plasma, CO_2 splitting is realized by electron impact and high temperature pyrolysis. As described in Section 2.1, high gas temperatures are also achieved by electronic elastic collisions. Therefore, the higher the electron density, the more collisions that occur, and the higher the conversion rate of CO_2. This has been verified by number of experiments with a cold, warm and thermal plasma, see Table 1, Fig. 6 and 13.

No matter what kind of plasma, plasma decomposes CO_2 into CO and O atoms. The reactions of neutral particles will occur simultaneously to bring the system into a chemical equilibrium. Fridman lists 16 relevant reactions (see his Table 5.1).[28] The most significant reactions are:

$$O + O + M \rightarrow O_2 + M \quad k_{R1} = 2.75 \times 10^{-34} \tag{R1}$$

$$CO + O + M \rightarrow CO_2 + M \quad k_{R2} = 6.54 \times 10^{-36} \exp(-2165/T_g) \tag{R2}$$

$$CO_2 + O \rightarrow CO + O_2 \quad k_{R3} = 7.7 \times 10^{-12} \exp(-16\,615/T_g) \tag{R3}$$

$$CO + O_2 \rightarrow CO_2 + O \quad k_{R4} = 1.23 \times 10^{-12} \exp(-12\,688/T_g) \tag{R4}$$

where, the rate coefficients are given in $cm^3\ s^{-1}$ and $cm^6\ s^{-1}$, for two-body and three-body reactions, respectively. M denotes a third body including all kinds of neutral particles in the reaction system like CO_2, CO or O_2. To qualitatively examine the contribution of these reactions, we take the density of M as 10^{18} cm^{-3} to turn k_{R1} and k_{R2} into two-body rates and compare them with the two-body rate coefficients for R3 and R4. The comparison R1–R4 as a function of temperature is shown in Fig. 2. In the estimate of the density we assumed the ideal gas law to be valid. A temperature beyond 3000 K is assumed. This may be an overestimate, and a density of 10^{19} cm^{-3} could be more appropriate. This would shift the curves for R1 and R2 an order of magnitude upwards.

At gas temperature lower than 800 K, k_{R1} is at least two orders larger than the others. This implies that the consumption of atomic oxygen in this temperature region is mainly through reactions of R1, which recombine O into O_2, and does not directly cause carbon monoxide production or loss. At temperature region of 800–2000 K, $k_{R4} > k_{R3}$, which implies that the reverse reaction caused by the molecular oxygen surpasses the reduction reaction of the atomic oxygen, resulting in an overall CO decrease. At temperatures higher than 2400 K the importance of various rates reverses: k_{R3} gradually exceeds k_{R4}, atomic oxygen may contribute to CO production, CO_2 pyrolysis is gradually prevailing.

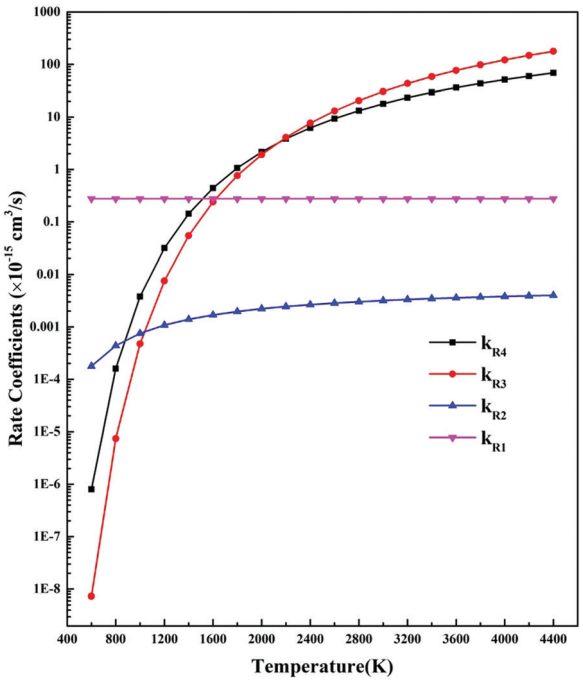

Fig. 2 The rate coefficients of free radical reactions *vs.* gas temperature in plasma. For comparison purposes, the rate coefficients of three-body reaction are multiplied by 10^{18} cm^{-3}, which is assumed to be the density of the third body.

According to the analysis above, for CO_2 decomposition in a cold plasma where the gas temperature is lower than 800 K and the electron temperature is high, the CO formed by electronic excitation will be retained, and one can harvest CO without worrying about CO recombination with atomic oxygen. In a warm plasma where the gas temperature is about 1500–3000 K, the CO formed by electronic and vibrational excitation can recombine with O_2; hence, a proper quench is needed. In a thermal plasma the conversion of carbon dioxide is driven by the joint effect of electron splitting and thermal reactions of neutral particles. This results in a higher conversion than if only one of the processes is active. Nevertheless, to obtain a significant final conversion rate, thermal quenching of the dissociated gas from their reaction temperature to about 800 K is required. In this way CO recombination with oxygen is avoided. The need for thermal quenching is a key problem that must be considered.

3. Pure CO_2 conversion by non-thermal plasma

In view of economics and the need for industrial application, the process of CO_2 conversion by plasma should have three characteristics simultaneously: (1) high CO_2 conversion rate, (2) high process energy efficiency, and (3) the possibility of large-scale production.

The conversion rate of a plasma process is defined as

$$x = \frac{CO_{2in} - CO_{2out}}{CO_{2in}} \quad (11)$$

The energy efficiency is defined as the ratio of chemical energy of CO harvested to the electrical energy spent,

$$\eta = \frac{\Delta H_{CO} Y_{CO}}{60P} \quad (12)$$

Here, CO_{2in} (mol min^{-1}) and CO_{2out} (mol min^{-1}) are the rates of CO_2 feed into and out of the plasma reactor, respectively, P (kW), is the plasma discharge power, ΔH_{CO}, the fuel value of CO (283 kJ $mole^{-1}$), and Y_{CO} (mol min^{-1}), the CO yield. These values will be discussed for the various types of plasma generators. The factor of 60 converts seconds into minutes.

3.1. The dielectric barrier discharge

The dielectric barrier discharge (DBD), also called silent discharge, was reviewed in detail by Kogelschatz in 2004.[30] Its main application is ozone synthesis in industry. The DBD plasma reactor used in CO_2 conversion is usually tubular, as shown in Fig. 3.

A high-voltage electrode is coaxially placed in a quartz tube wrapped in a grounded electrode. The gap between high-voltage electrode and quartz tube is several millimeters. By suppling an alternating high voltage (more than 1000 V) on the two electrodes, a discharge is created and the gas flowing through the discharge tube is dissociated. The quartz dielectric prevents the formation of sparks and arcs in the plasma tube. In operation the plasma current flows in channels at atmospheric pressure. The channels are characterized by a number of micro-discharge filaments of 0.1–0.2 mm in diameter and with a mutual distance of order a few millimeters. The DBD plasma reported in CO_2 conversion is usually operated at high electric field strength, with discharge power about hundred Watts and CO_2 feed is tens of milliliters per minute. It is a typical cold plasma with high electron temperature, low mean electron density and gas temperature in reaction space, as shown in Table 1. There is a large literature on CO_2 splitting

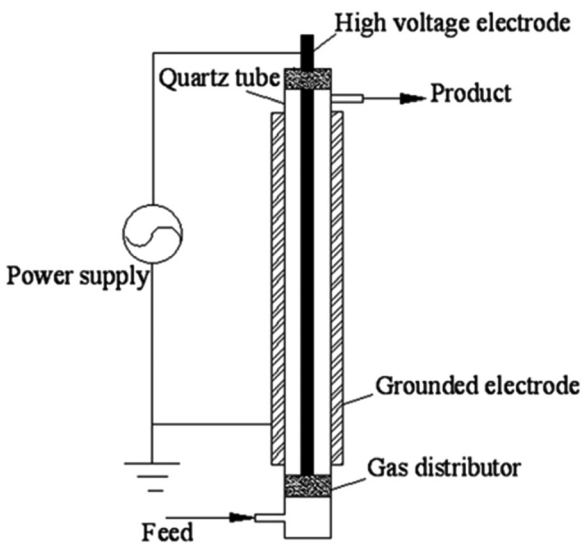

Fig. 3 Schematic of a DBD reactor. Reaction gas is fed in on the lower left and the product gas emerges from the top right.

by DBD's. The results are reviewed at several places, and will be discussed later.[20,23,25,31,32] Recent entries to the literature include ref. 33–36.

3.2. Gliding arc discharge

The gliding arc (GA) discharge, which operates at atmospheric pressure, was patented by Lesueur *et al.* in 1988, see ref. 37. The early GA generator (Fig. 4) consists of one or more pairs of electrodes placed face to face. The electrodes are separated by a gap that increases along the flow direction. Appling a high voltage on the electrodes, an arc is ignited at the closest gap. The arc is elongated as the arc root glides along the surface of electrodes due to the fast flow of working gas. The plasma extinguishes downstream at the widest gap and new discharges immediately appear at the initial spot repeatedly.[20,28]

A new type of GA discharge is based on hollow cylindrical electrodes placed vertically with a tangential gas inlet, as shown in the right part of Fig. 4. It was developed at Drexel University by Nunnally *et al.*[39] The inner diameter of the anode is smaller than that of cathode. The gas flow enters through a tangential inlet in the midplane, resulting in an upward vortex. When the spiraling gas arrives at the top of the cathode, it will reverse to form an internal, smaller diameter swirl flow downwards toward the outlet of anode nozzle. When a direct-current high voltage is applied, an arc is ignited at the closest distance between cathode and anode. The arc root at cathode then glides to the top of cathode by the drag of spiraling gas to form a central arc surrounded by an upward vortex.

The GA plasma reported in CO_2 conversion is operated also at ambient pressure; its physical characters depend on the discharge power and the gas flow rate. Usually, the discharge power is about 1000 W, and a CO_2 feed of 10–20 L min^{-1} is required to form the gliding vortex. It results in a GA plasma with a 1–2 eV electron temperature, an electron density of about 10^{12} cm^{-3} and gas temperature of 1500–3000 K in the reaction volume.[38] Therefore, it belongs to warm plasma as shown in Table 1. In some cases much higher electron densities (10^{17} cm^{-3}) have been obtained in gliding arcs.[40] The work with gliding arc plasmas has been reviewed extensively.[20,25,32] Recent studies include ref. 41–43.

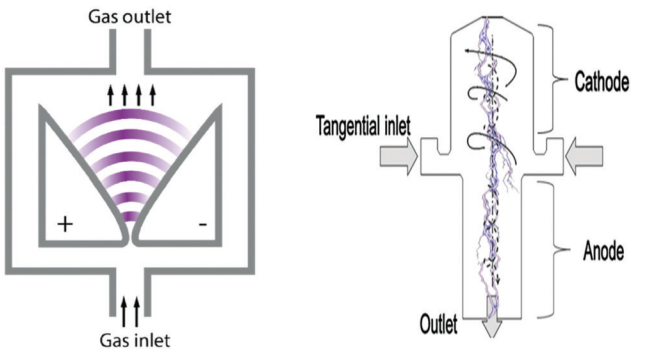

Fig. 4 Schematics of Gliding Arc discharges. From ref. 20 and 38. Reproduced with permission.

3.3. Microwave (MW) discharge plasma

The Microwave (MW) discharge plasma is produced by electromagnetic induction. As shown in Fig. 5, a MW plasma reactor consists of a quartz tube, inserted into a microwave cavity powered by MW generator with a frequency of a few GHz. When MW power is introduced through the wave guide into the cavity, the gas flowing through the quartz tube is excited to form plasma. At reduced pressure (less than 0.1 atm), a MW discharge produces a warm plasma with electron temperature, mean electron density and gas temperature comparable to that of a GA. However, at atmospheric pressure, MW and RF discharges produce a thermal plasma.

3.4. Conversion rate and energy efficiency

The conversion rate and energy efficiency achieved in experiments of pure CO_2 conversion by cold and warm plasma process have been summarized by Snoeckx and Bogaerts.[20] Adopting these data we compiled Fig. 6 for comparison of CO_2 conversion by the various plasma generators discussed.

Combining Table 1 and Fig. 6, the conversion rate and energy efficiency that can be achieved simultaneously are closely related to electron density (or the type of plasma) and quenching means used. In a cold plasma such as DBD, both conversion rate and energy efficiency are low because of low electron density and the use of the electronic excitation mechanism. DBD plasma did not employ some quenching method. It is simple to operate a DBD and no expensive pumping systems are required. Fig. 6 demonstrates that in warm plasma such as a gliding arc, there is higher energy efficiency than DBD but a low conversion rate because of the moderate electron density and self-quenching with a large CO_2 flow. Another reason of the low conversion rate may be the limited fraction of gas passing through the arc, hence the limited gas residence and excitation time in the arc, as indicated by modeling.[42,44] In a warm plasma such as MW and RF, there are either high energy

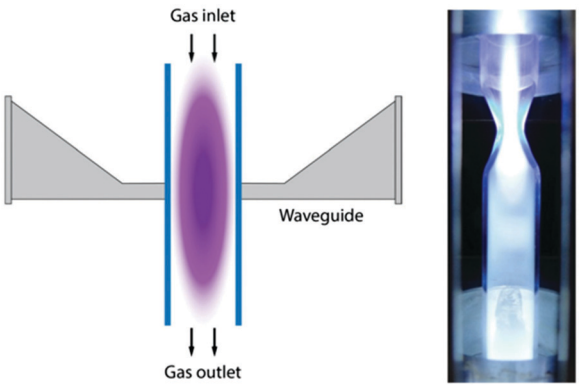

Fig. 5 Schematic of a MW plasma generator for CO_2 conversion (left). MW power is provided by the waveguide indicated. The gas flows through the tube from top to bottom. In the right hand figure, a section through a more complex MW system is given, using a nozzle or constriction for the flow. The typical discharge power for MW plasma reported in CO_2 conversion is 300–1000 Watts, and CO_2 feed of ~10–20 L min^{-1}. See ref. 20. Reproduced with permission.

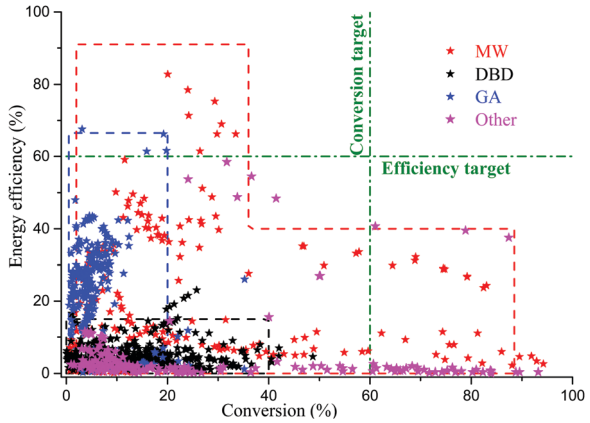

Fig. 6 CO_2 conversion and energy efficiency achieved in different plasma experiments. The data points represent the results. Black: labeled DBD: dielectric barrier discharge; Blue: labeled GA: gliding arc; Red: labeled MW: Microwave and radiofrequency plasma. Most data redrawn from ref. 20. To give an indication of the performance we have drawn green dash-dotted lines to represent an efficiency and a conversion target, both set at 60%. The efficiency target is taken from the value given in Fig. 24 of ref. 20. The conversion efficiency we took at 60% because several studies mentioned in the review show that this value can be obtained and exceeded; see also the discussion on page 5826 of ref. 20.

efficiency and low conversion rate, or low energy efficiency and high conversion rate, because of the moderate electron density and (some level of) supersonic expansion quenching when reaction effluent flows out of the plasma reactor. There is more recent work, not included in Fig. 6, but cited earlier in the text. These recent studies do not change the overall picture provided in Fig. 6.

None of the data shown in Fig. 6 shows both high conversion rate and high energy efficiency; there are no points in the upper right quadrant of Fig. 6. However, as we will discuss in the next section, it is possible to achieve high conversion rate and high energy efficiency using a thermal plasma with chemical quenching.

In addition to energy efficiency and conversion rate, another question for CO_2 conversion by plasma is the possibility of large production capability. This is related not only to the size of the plasma reactor itself and the product flow. In addition, the separation of the components of the dissociated gas (CO_2, CO, O_2) produced in the plasma reactor need to be considered. For pure CO_2 conversion, even if all or most of the feed is converted eliminating CO_2, the separation of CO and O_2 is still a technical challenge today since its energy cost is even higher than that of the splitting process.[45] Therefore, for industrial application, development of a plasma process with high energy efficiency and conversion rate, flexible operating scale and a process that bypasses the separation step is highly desirable and will give the most competitive process. These goals can be achieved by a process using a thermal plasma for CO_2 conversion with chemical quenching, to be discussed in the next section.

Very recently it has been demonstrated that membranes have been developed that can separate CO and O in the reactor.[46] This would eliminate the need for a separate gas separator and yield a stream of almost pure CO. This interesting development would open new opportunities for CO_2 conversion by plasma. In our work, described in Section 5, there is no need for a separator.

4. Pure CO_2 conversion by a thermal plasma

As shown in Table 1 a thermal plasma is produced at atmospheric or higher pressure and the electron density in a thermal plasma is higher than that in a cold or warm plasma. By frequent electronically elastic collisions, the electrons transfer the energy received from the electric field to heat heavy particles. It leads to a very high temperature of the heavy particles, close to that of electrons; both in the order of thousands K. Therefore, chemical reactions in thermal plasma are both electron-induced reactions and thermo-chemical reactions.

4.1. Generation of thermal arc plasma.

There are several types of atmospheric thermal plasma devices, reviewed by Fauchet and Vardelle,[47] and in the book by Fridman.[28] A recent application to RF heating of an atmospheric CO_2 plasma is given by Spencer and Gallimore.[48,49] The DC arc generator is the most used one. As shown in Fig. 7,[47] a DC arc generator consists of a tungsten cathode and a copper cylindrical hollow working anode. Between them there may be some copper cylindrical hollow segments called floating electrodes. All the electrodes are water-cooled, coaxially mounted, and separated by insulating materials. From the gaps between adjacent electrodes, the discharge gas is feed in.

The arc is initiated between cathode and working anode by a high-voltage (several kV) trigger, and maintained by a continuous DC voltage of several hundreds of Volts. Due to continuously feeding of discharge gas, the arc is pushed out of the working anode nozzle, resulting in a high temperature flame torch. The power of the torch can reach 1–10^4 kW by controlling the input voltage or current.

The thermal arc used recently by the authors is shown in Fig. 8a.[50] The device consists of a cathode chamber with Ar gas inlet 1 for starting and maintaining the discharge and protecting the cathode from carbon contamination by CO_2. The arc flows into a second chamber with gas inlet 2 to inject CO_2 in the plasma flow. The cylindrical anode is positioned at the end of this second section. Below the exit of chamber 2 the plasma

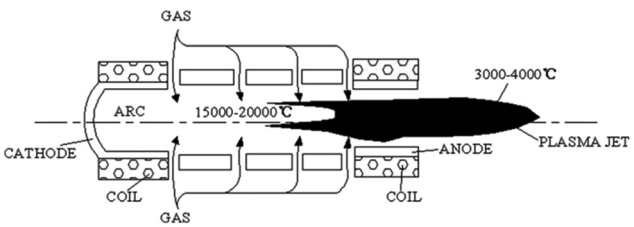

Fig. 7 Schematic of a DC thermal plasma device.

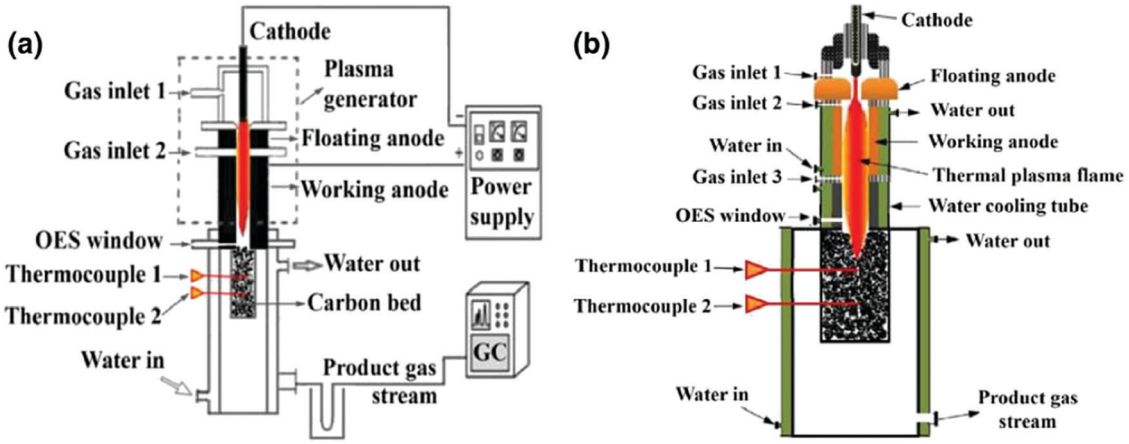

Fig. 8 (a) Thermal arc for CO_2 conversion. In (b) an extension to this thermal arc is shown, where a gas can be seeded into the plasma flow before entering the carbon bed. See text.

flows into a carbon bed with two thermocouples in a water-cooled chamber. The product gas leaves the device at the bottom and is analyzed with a gas chromatograph. In experiments with typical arc powers of 10 kW the flows of Ar, CO_2 (and N_2 when used) are the same. For an arc running at 100 kW the Ar flow is much lower than the CO_2 flow. We have not tried to study the effect of Ar in detail. A photograph of the arc source running at 100 kW is shown in Fig. 9.

It is interesting to mention that thermal arcs have been used extensively as flexible, controllable and tunable heating source in industry worldwide.[47,51–54] Applications include cutting, welding, thermal spraying of various materials, production of carbon black and hydrogen from hydrocarbons.

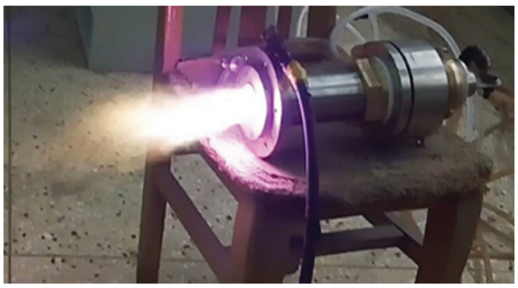

Fig. 9 Photograph of a 100 kW atmospheric thermal arc source in operation in the lab of the authors.

4.2. CO_2 conversion by thermal arc plasma

The experimental exploration of CO_2 conversion by thermal plasma has begun in the late nineteen sixties.[52] Most developments are described in Fridman's book.[28] In these early experimental approaches,[55] shown in Fig. 10, Ar was used as discharge gas to form plasma flame torch, and CO_2 was injected into the torch after the anode nozzle. A movable water-cooled heat exchanger was used for quenching the dissociated gas. The temperatures and composition of the partially dissociated gas could be sampled by thermocouples and probes in the heat exchange channel. Experimental results for three different Ar/CO_2 ratios are plotted in Fig. 11.[55]

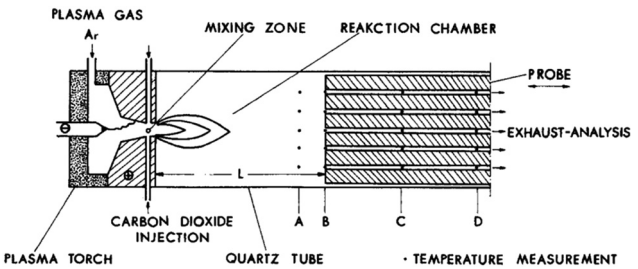

Fig. 10 Schematic of an early experimental setup for CO_2 conversion by thermal plasma. From ref. 55. Reproduced with permission.

Considering the discharge power and the electro-thermal conversion efficiency of plasma generator, the enthalpy changes of the reaction system before and after reaction, the mean (initial) temperature of the dissociated gas can be calculated self-consistently by energy balance and thermodynamics. In most experiments, it is over 3000 K, the domain of pyrolysis. Assuming the pyrolysis was at equilibrium, the CO_2 conversion rate before quenching will be over 50% according to Fig. 1. Unfortunately, the measured CO_2 conversion after quenching by a water-cooled heat exchanger is not more than 35% for the system referred to by Fig. 11. The loss in conversion takes place in the quenching phase, where the back-reaction $O + CO \rightarrow CO_2$ reduces the yield. Huczko and Szymanski showed that the maximum quenching rate from 3000 K to 1500 K conducted by water-cooled heat exchanger was no more than 4×10^6 K s^{-1}.[55,56] It is too low to completely "freeze" the dissociation product. Vermeiren and Bogaerts carried out an extended modelling study of quenching of the CO_2 plasma under a number of conditions.[57] Quenching rates changing 6 orders of magnitude are studied. Depending on conditions quenching can increase the conversion by more than a factor of three. Methods to realize the quenching are briefly discussed. Conditions studied differ from the ones prevalent in thermal arcs.

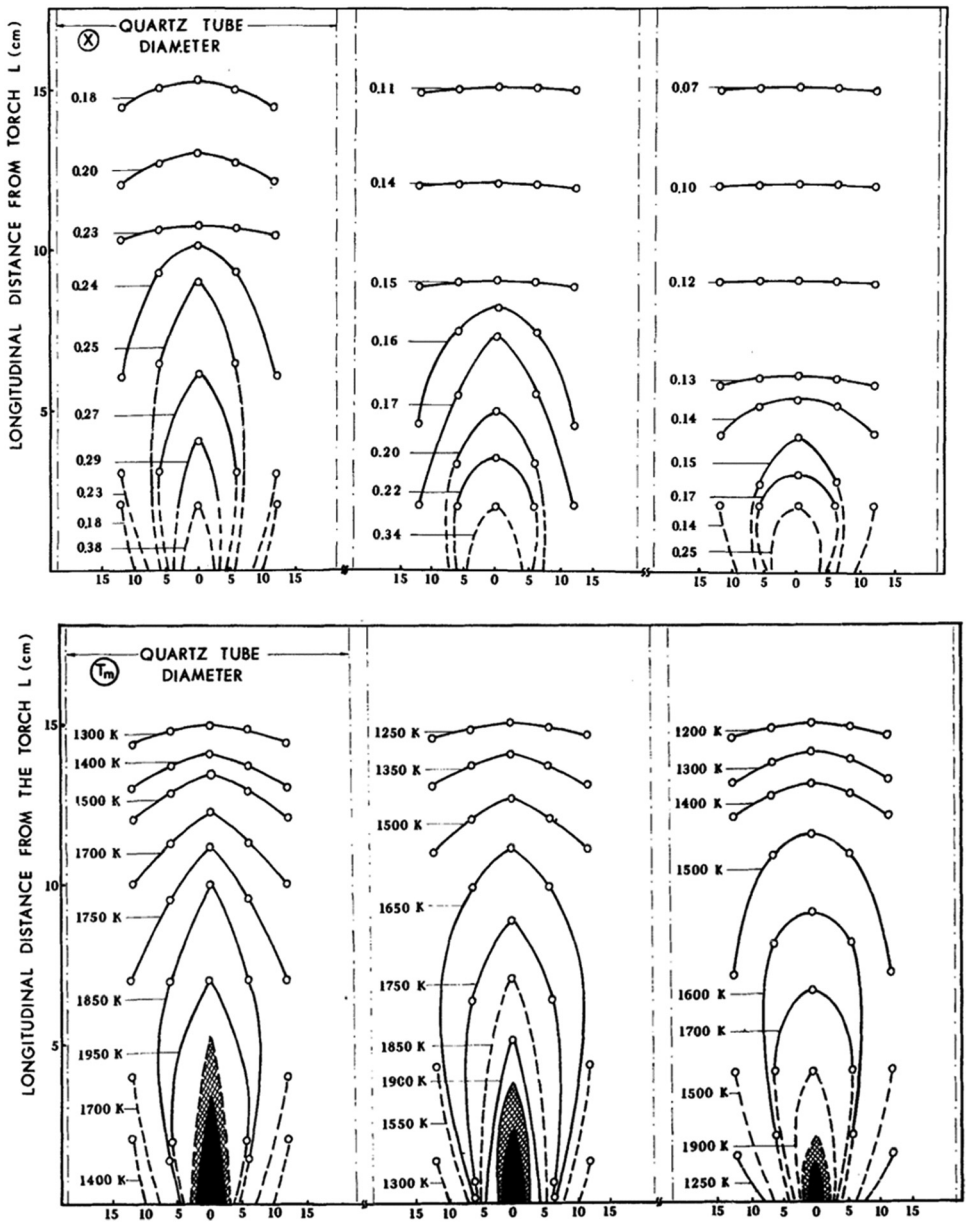

Fig. 11 The Spatial distribution of the temperature of the partially dissociated gas (upper panels) and CO_2 conversion rate (lower panels) in early experiments. The rapid decrease of the temperatures demonstrates the importance of quenching. Data for CO_2 feed flows of 3.7×10^{-3} mole s^{-1}, 8.1×10^{-3} mole s^{-1}, 1.3×10^{-2} mole s^{-1}. data are from ref. 55. Reproduced with permission.

Li *et al.* provided a novel quenching method based on the synergy between a supersonic expansion of the CO_2 plasma and a water-cooled heat exchanger.[58] Li *et al.* used a working anode designed as a contraction nozzle, and the dissociated gas was automatically pumped from plasma region at supersonic speeds into a water-cooled heat exchanger. It brings about the final CO_2 conversion of 40% and the corresponding energy efficiency of 18% were obtained in experiments. Yang and Yin did a chemical kinetic simulation for the quench process.[59] Quenching rates changing over 5 orders of magnitude are found. The results shown in Fig. 12 indicates that taking the CO_2 thermodynamic equilibrium conversion rate at temperature of 3050 K to be 54%, the results vary greatly with assumed quenching rate; the higher the quench rate, the greater the retained CO_2 conversion rate. Furthermore, a computational fluid dynamics (CFD) simulation with the configuration in ref. 55 revealed that a quenching rate of 10^7 K s^{-1} could be expected to cool the dissociated gas from more than 3000 K to 1000 K.[59] It is consistent with the 45% CO_2 conversion rate obtained in the experiments.

Physical quenching does significantly increase the conversion, but it remains far below an efficiency target of 60% drawn in Fig. 6.

4.3. CO_2 conversion by thermal plasma with chemical quenching

According to the analysis above, for CO_2 conversion by a thermal plasma, two conditions must be met: the target product generated

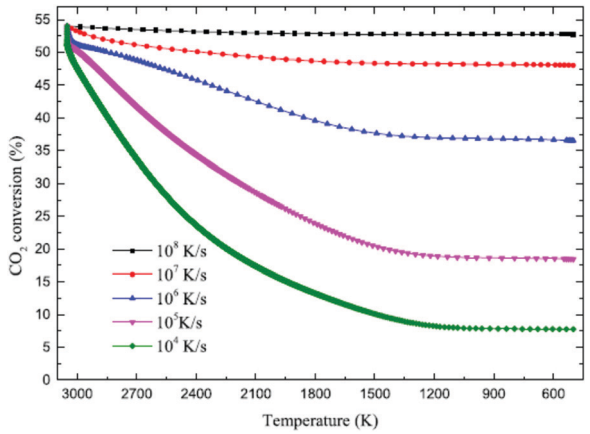

Fig. 12 Computed final conversion rate of CO_2 at quenching rates of 10^8, 10^7, 10^6, 10^5, and 10^4 K s^{-1}. The initial conversion in the plasma reactor is taken to be 54%, see Fig. 1.

in the high temperature reactor must not be consumed during the quenching process, and the product generated in the quenching process must be preferably pure energetic chemical compounds without CO_2 and O_2 in the product stream. All methods discussed so far produce O_2 as a byproduct and, with these methods, an expensive separation step of CO and O_2 is required.[45] So, we note that the physical quenching, discussed in the last paragraph is not enough.

Since physical quenching is not sufficient, we consider "chemical quenching". In chemical quenching, O radicals and O_2 molecules are rapidly removed when reactant flows out of high temperature reactor by a chemical reaction. A possibility is to add gasses like CH_4 or H_2 to react away the atomic O from the reaction $CO_2 \rightarrow CO + O$. This has been demonstrated for the first time by Aerts *et al.* who showed that addition of a few percent of H_2 or CH_4 strongly suppressed the formation of O_2 through the formation of H_2O. The study was carried out in a DBD and the conversion was only a few percent.[60] For thermal arcs, the addition of H_2 does indeed significantly increase the conversion of CO_2 under otherwise similar conditions (unpublished results for both RF plasma and thermal arcs). Further analysis of that data is necessary.

Adding H_2 on an industrial scale adds an additional complication. H_2 would have to be prepared at additional cost with H_2O and CH_4 as main products. For CH_4 addition the situation is quite different. The reaction of CO_2 with CH_4 is called dry reforming of methane (DRM), which has been extensively studied. The available literature has been reviewed several times.[20,23,25,61–64] The Sichuan University group has demonstrated that very high conversions (close to 90%) with high selectivity towards CO and H_2 (up to 80%) can be obtained.[23,31,59,64–68] The amount of O_2 is not mentioned in the papers but will be low given the high conversion of CO_2 and the high selectivity towards CO. We do not want to enter into any further discussion here, because the work on DRM has been reviewed elsewhere and this paper focuses on the conversion of pure CO_2. For an efficient conversion by thermal plasma, one needs to quickly quench the reaction products from the arc with a rate more than 10^6 K s^{-1}, to remove the free oxygen from the flow.

5. CO_2 conversion using solid carbon

Besides reacting the excess oxygen away with a gas like CH_4 it is also possible to do this using a solid reactant. It should be mentioned that in addition a solid in the plasma reactor can act as a catalyst. In the case of DRM it has been shown that adding a catalyst does increase the conversion.[31,64,65] Carbon has been tried recently as a solid reactant.

The composition of the flow at the exhaust of a thermal CO_2 arc is not self-evident. Two processes contribute: thermal pyrolysis and dissociation induced by slow electrons. The exhaust flow thus will contain CO_2, CO, O_2 and O. For pyrolysis at 3000 K (see Fig. 1) and considering the elementary balance the proportion is about 50 : 50 : 21 : 8. Electron induced processes will boost CO and O.

The CO_2 plasma exhaust with temperatures more than 3000 K will easily react with carbon according to the following reactions:

$$C(s) + O(g) \rightarrow CO(g) \quad (13a)$$

$$2C(s) + O_2(g) \rightarrow 2CO(g) \quad (13b)$$

$$C(s) + CO_2(g) \rightarrow 2CO(g) \quad (13c)$$

The first two reactions are strongly exothermic combustion reactions, and the third reaction is the strongly endothermic Boudouard reaction.[27] The former can quickly remove free oxygen in the pyrolysis gas, and the later can rapidly cool the pyrolysis gas, so both should contribute to preventing the reverse reaction. At the same time, these reactions produce new CO while suppressing the reverse reaction. Therefore, adding C at the end of the flow is thus expected to increase the CO yield and reduce the other components of the exhaust gas. This is indeed what has been observed.[69] Our results are given as additional red points added to on the overview prepared by Snoeckx and Bogaerts,[20] shown in Fig. 13. Our data refers to experiments with the thermal arc shown in Fig. 8a with flows for Ar and CO_2 of about 25 slm and arc powers around 10 kW.[69] The red points represent measurements with different flow or power conditions.

Most data shown in Fig. 13 refers to the use of pure CO_2. Our data obtained with a thermal arc refers to a plasma consisting of a 1–1 mixture of Ar and CO_2. The Ar is required to protect the cathodes of the thermal arc. In the present experiment the flow of Ar is the same as the CO_2 flow. However, when we scale up the device, such as shown in Fig. 9, the Ar flow will be much smaller than the CO_2 flow. Therefore, Ar is mainly a carrier gas, that does not participate in the CO_2 splitting. Therefore, in the calculation of the conversion, we take the ratio of the outgoing and incoming CO_2 flow (eqn (11)) and the fraction of Ar does not enter. In the calculation of the power imparted on the CO_2 we take the total plasma power. This would imply that all power

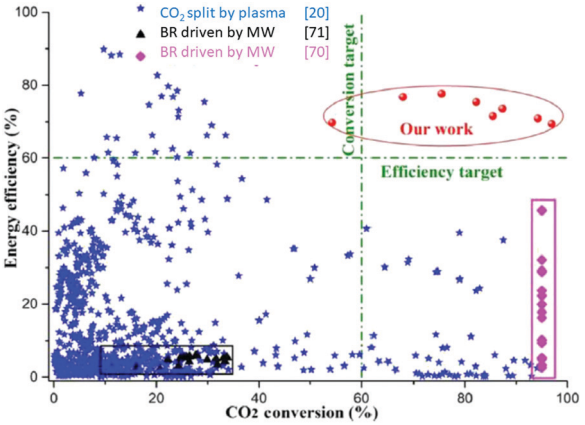

Fig. 13 Overview of the energy efficiency of all data on CO_2 available as a function of the CO_2 conversion. In blue are the data points compiled by Snoeckx and Bogaerts,[20] also shown in Fig. 6; red are data by the Yin group using a thermal arc and a solid C target;[50,69] purple are the results by Bermudez *et al.*[70] using the Boudouard reaction driven by microwave heating of a solid C reactant in a CO_2 flow; black are the data on the Boudouard reaction driven by microwave or thermal heating of solid C by Hunt *et al.*[71]

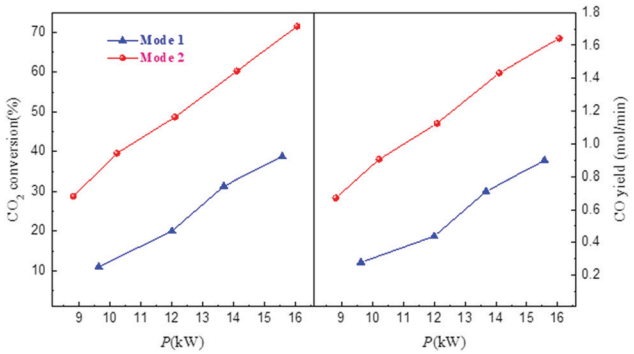

Fig. 14 CO_2 conversion and CO yield in triple flow experiments operated in two different modes discussed in the text.

to ionize Ar is transferred to CO_2, which is unlikely. Therefore, the value of the energy efficiency given is an underestimate.

It is seen that our work does meet the efficiency and conversion targets indicated. Furthermore, although not shown in the figure, there is no O_2 in the product flow. The final product consists of only CO and CO_2 and thus no expensive separation step is needed to separate CO and O_2.

The data by Bermudez *et al.* and Hunt *et al.* in Fig. 13 are taken for the pure Boudouard reaction without using a plasma.[70,71] The experiment by Bermudez was arranged such that the conversion was always 95% while varying heating power and flow.[70] The data by Hunt *et al.* show a much lower conversion, but are carried out at lower power levels than Bermudez *et al.*[71] The figure shows that adding a plasma step in the Boudouard reaction significantly increases the energy efficiency. There can be two reasons for this. Firstly, in the plasma Boudouard reaction, the carbon dioxide is first heated and cracked and then applied to the solid carbon surface where reactions 13a and 13b occur, in addition to 13c, while in the thermal Boudouard reaction, the solid carbon is first heated and then CO_2 with room temperature applied to the carbon surface. Alternatively, the plasma increases the production of O atoms and O_2 molecules in the flow that react in exothermic reactions 13a and 13b with C, enhancing the yield. In the experiments, no O_2 is detected in the final product stream, and the amount of CO harvested is about two times of the CO_2 converted. It implies that the free oxygen from CO_2 splitting as shown in Fig. 1 have been completely reacted with carbon. Therefore, plasma drives dissociation beyond the thermal Boudouard reaction. These questions will be further examined by additional experiments, described in the next paragraph.

In order to examine the role of the plasma, experiments with triple gas flows (Ar, CO_2, N_2) have been carried out with the arrangement shown in Fig. 8b.[50] In experiments labeled Mode 1 in Fig. 14 Ar is injected through gas inlet 1, N_2 through inlet 2 and CO_2 through inlet 3. In experiments labeled Mode 2 in Fig. 14 Ar is injected through gas inlet 1, CO_2 through inlet 2 and N_2 through inlet 3. The idea is that in mode 1 CO_2 is not injected in the plasma and only heated by the hot N_2 gas stream from the arc, while in mode 2 CO_2 is 'treated' by plasma. In Fig. 14 it is shown that Mode 2 exhibits a much higher conversion than Mode 1, while temperature measurements show a very similar heating of the C layer for both experiments. So, pretreating the CO_2 by the plasma increases the conversion significantly, and the Boudouard reaction is not only driven thermally.

To study the effect of plasma excitation of CO_2 further the experiments with the Boudouard reaction have been extended using a RF discharge. The equipment used has been described earlier in a number of papers.[26,50,72–77] In some of these experiments catalysts were placed in the reactor inside the RF coils.[76] In the same way as for the catalysts we have inserted carbon, confined by a Cu mesh. In these experiments the power levels (typically 50–400 W) and operation pressures (typically 100 Pa) are much lower than for the thermal arcs. Details of these experiments will be given elsewhere.[78] The point of this investigation is to what extend a carbon surface is reactive towards a CO_2 plasma at temperatures where the thermal Boudouard reaction does not run. The most important results are shown in Fig. 15, where the CO_2 conversion as a function of RF power is seen for three cases: two with C pellets and one with an empty RF reactor. Clearly adding C increases the conversion significantly. In this experiment the temperature of the C could be measured by a pyrometer. The C temperature never exceeded values of 800 K, far below the operation temperature of a thermal Boudouard reaction. So, a chemical reaction takes place at the carbon surface, that is not the regular Boudouard reaction. The reaction of O + C → CO is an obvious candidate to cause the increased CO production. We have measured the weight loss of the carbon in the reactor and noticed that in extended runs carbon is removed from the solid carbon samples. The removal of O also decreases the probability of recombination of CO and O to form CO_2.

From these experiments we have learned that plasma 'treated' CO_2 does react with carbon at low temperatures and in this

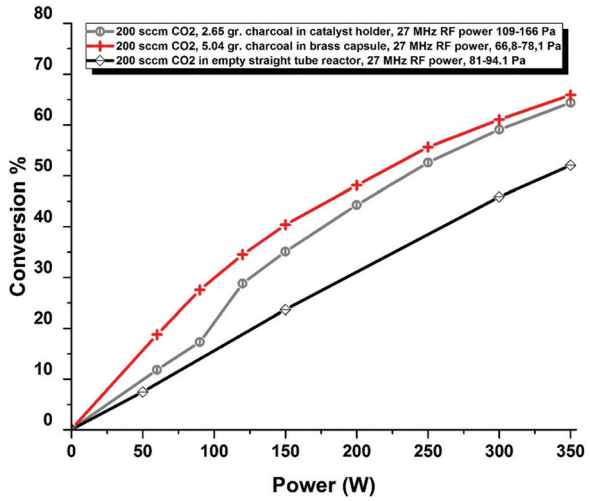

Fig. 15 CO_2 conversion in an RF plasma as a function of RF power. Red + and black circles show results with charcoal in a holder, open diamonds show results for an empty reactor without any C. From ref. 78.

way increases the CO yield from this RF reactor. We note that the role of the carbon is not that of a catalyst, because the carbon is consumed in the reaction. It is interesting to note that in reactions of energetic O-atoms from a molecular beam with vitreous carbon surfaces a number of surface reactions leading to mainly CO, but also CO_2 and O_2 has been observed.[79] So carbon surfaces are reactive with respect to O-atoms. The connection between these different classes of experiments needs further analysis.

By the experiments with atmospheric thermal arcs it could be demonstrated that using carbon at the exhaust of a thermal CO_2 plasma arc the energy efficiency and conversion could be enhanced to values that are industrially viable. Recent experiments in our laboratory have demonstrated that thermal arcs with powers up to 100 kW can be operated in steady state. A picture of one of the first 100 kW arcs is shown in Fig. 9. Clearly its size is not prohibitive for industrial application.

5.1. Perspective for CO_2 conversion by plasma driven Boudouard reaction

The results presented in this section demonstrate that reacting the flow from a 10–100 kW CO_2 thermal arc with a carbon surface yields remarkably high values for energy efficiency and conversion. In addition, there is no O_2 in the product flow. These are excellent conditions for conversion of CO_2 into CO.

The CO generated can be used for combustion or serve as input for a Fisher–Tropps reaction.

6. Conclusions

CO_2 conversion is an important process in view of the large emission of this gas from various point sources, such as coal or gas fired electrical power plants. Conversion should be done using sustainably generated electrical power and allow for the intermittent character of sustainable electricity generated by solar or wind. Our thermal arc can be switched on and off very quickly, and stable operation is obtained in a few minutes. So they are compatible with intermittent power.

In this paper we introduce plasma processing as a possible conversion method and discuss the various mechanisms in which plasma can activate and dissociate CO_2. Several plasma generation methods are discussed. Thermal arcs appear to be a very interesting option, because they work at atmospheric pressure and have a large throughput. Recombination of CO and O in the exhaust flow is the main limitation of the CO_2 conversion. When using carbon at the exhaust of the thermal arc very high conversions and energy efficiencies can be obtained. The reactor produced almost exclusively CO without O_2, eliminating the need for a CO/O_2 separation step. Disadvantages of this method is that additional carbon is required and that cathodes are used, which have a limited lifetime. Much research is needed to turn atmospheric arcs with a carbon reactor into an industrially viable device. The potential is clearly there.

Although the approach of this research is mainly experimental and done in an engineering fashion, the input of atomic and molecular physics and of surface science is very valuable. Spectroscopy gives significant additional information on the plasma and surface analysis of catalysts and solid reactants can lead to mechanistic information on the microscopic operation of these plasma devices. When developing this CO_2 conversion process further, there is a very interesting field of research ahead of us, that should take full advantage of the detailed knowledge generated on the underlying mechanisms by the fields of atomic and molecular physics and surface science.

Specifically, research on CO_2 conversion by plasma should employ more diagnostic tools, such as various laser spectroscopies, *in situ* operandi surface analysis, and advanced plasma analysis. Obviously, advanced modelling should accompany experimental work. Upscaling to power levels of 100 kW or more will tell us if plasma technology will be viable for industrial applications, and to fight climate change on a higher level of plasma and conversion intensity.

Conflicts of interest

There are no conflicts to declare.

References

1 I. A. G. Wilson and P. Styring, *Front. Energy Res.*, 2017, **5**, 10.
2 A. Delparish and A. K. Avci, *Fuel Process. Technol.*, 2016, **151**, 72–100.
3 C. Graves, S. D. Ebbesen, M. Mogensen and K. S. Lackner, *Renewable Sustainable Energy Rev.*, 2011, **15**, 1–23.
4 K. Matsumoto, *PLoS One*, 2015, **10**, 17.
5 P. Hartley, K. B. Medlock, T. Temzelides and X. Y. Zhang, *Energy J.*, 2016, **37**, 233–290.
6 B. Shakouri and S. K. Yazdi, *Energy Sources Part B*, 2017, **12**, 838–845.

7 J. M. Lavoie, *Front. Chem.*, 2014, **2**, 17.
8 Y. Hao and A. Steinfeld, *Sci. Bull.*, 2017, **62**, 1099–1101.
9 C. F. Shih, T. Zhang, J. H. Li and C. L. Bai, *Joule*, 2018, **2**, 1925–1949.
10 J. D. Hunt, B. Zakeri, R. Lopes, S. Paulo, A. Nascimento, N. J. de Castro, R. Brandao, P. S. Schneider and Y. Wada, *Renewable Sustainable Energy Rev.*, 2020, **129**, 14.
11 T. Ma, H. X. Yang and L. Lu, *Energy Convers. Manag.*, 2014, **79**, 387–397.
12 M. Carmo, D. L. Fritz, J. Merge and D. Stolten, *Int. J. Hydrogen Energy*, 2013, **38**, 4901–4934.
13 A. Navarrete, G. Centi, A. Bogaerts, A. Martin, A. York and G. D. Stefanidis, *Energy Technol.*, 2017, **5**, 796–811.
14 E. V. Kondratenko, G. Mul, J. Baltrusaitis, G. O. Larrazabal and J. Perez-Ramirez, *Energy Environ. Sci.*, 2013, **6**, 3112–3135.
15 Y. Izumi, *Coord. Chem. Rev.*, 2013, **257**, 171–186.
16 J. Albo, M. Alvarez-Guerra, P. Castano and A. Irabien, *Green Chem.*, 2015, **17**, 2304–2324.
17 Y. Y. Birdja, E. Perez-Gallent, M. C. Figueiredo, A. J. Gottle, F. Calle-Vallejo and M. T. M. Koper, *Nat. Energy*, 2019, **4**, 732–745.
18 R. J. Detz, K. Sakai, L. Spiccia, G. W. Brudvig, L. C. Sun and J. N. H. Reek, *ChemPlusChem*, 2016, **81**, 1024–1027.
19 R. J. Detz, J. N. H. Reek and B. C. C. van der Zwaan, *Energy Environ. Sci.*, 2018, **11**, 1653–1669.
20 R. Snoeckx and A. Bogaerts, *Chem. Soc. Rev.*, 2017, **46**, 5805–5863.
21 A. Bogaerts, T. Kozak, K. van Laer and R. Snoeckx, *Faraday Discuss.*, 2015, **183**, 217–232.
22 A. Bogaerts and G. Centi, *Front. Energy Res.*, 2020, **8**, 23.
23 X. M. Tao, M. G. Bai, X. A. Li, H. L. Long, S. Y. Shang, Y. X. Yin and X. Y. Dai, *Prog. Energy Combust. Sci.*, 2011, **37**, 113–124.
24 A. Bogaerts and E. C. Neyts, *ACS Energy Lett.*, 2018, **3**, 1013–1027.
25 W. C. Chung and M. B. Chang, *Renewable Sustainable Energ. Rev.*, 2016, **62**, 13–31.
26 E. Devid, D. Y. Zhang, D. P. Wang, M. Ronda-Lloret, Q. Huang, G. Rothenberg, N. R. Shiju and A. W. Kleyn, *Energy Technol.*, 2020, **8**, 10.
27 P. Lahijani, Z. A. Zainal, M. Mohammadi and A. R. Mohamed, *Renewable Sustainable Energy Rev.*, 2015, **41**, 615–632.
28 A. Fridman, *Plasma Chemistry*, Cambridge University Press, New York, 2008.
29 M. A. Lieberman and A. J. Lichtenberg, *Principles of Plasma Discharges and Materials Processing*, Wiley-Interscience, 2005.
30 U. Kogelschatz, *Plasma Phys. Control. Fusion*, 2004, **46**, B63–B75.
31 D. H. Li, X. Li, M. G. Bai, X. M. Tao, S. Y. Shang, X. Y. Dai and Y. X. Yin, *Int. J. Hydrogen Energy*, 2009, **34**, 308–313.
32 B. Ashford and X. Tu, *Curr. Opin. Green Sustain. Chem.*, 2017, **3**, 45–49.
33 B. Ashford, Y. L. Wang, C. K. Poh, L. W. Chen and X. Tu, *Appl. Catal., B*, 2020, **276**, 10.
34 D. H. Mei and X. Tu, *ChemPhysChem*, 2017, **18**, 3253–3259.
35 D. H. Mei, B. Ashford, Y. L. He and X. Tu, *Plasma Process. Polym.*, 2017, **14**, 13.
36 D. H. Mei, S. Y. Liu and X. Tu, *J. CO2 Util.*, 2017, **21**, 314–326.
37 C. S. Kalra, Y. I. Cho, A. Gutsol, A. Fridman and T. S. Rufael, *Rev. Sci. Instrum.*, 2005, **76**, 7.
38 M. Ramakers, G. Trenchev, S. Heijkers, W. Z. Wang and A. Bogaerts, *ChemSusChem*, 2017, **10**, 2642–2652.
39 T. Nunnally, K. Gutsol, A. Rabinovich, A. Fridman, A. Gutsol and A. Kemoun, *J. Phys. D: Appl. Phys.*, 2011, **44**, 7.
40 X. Tu and J. C. Whitehead, *Int. J. Hydrogen Energy*, 2014, **39**, 9658–9669.
41 W. Z. Wang, D. H. Mei, X. Tu and A. Bogaerts, *Chem. Eng. J.*, 2017, **330**, 11–25.
42 S. R. Sun, H. X. Wang, D. H. Mei, X. Tu and A. Bogaerts, *J. CO2 Util.*, 2017, **17**, 220–234.
43 S. R. Sun, S. Kolev, H. X. Wang and A. Bogaerts, *Plasma Sources Sci. Technol.*, 2017, **26**, 12.
44 M. Ramakers, J. A. Medrano, G. Trenchev, F. Gallucci and A. Bogaerts, *Plasma Sources Sci. Technol.*, 2017, **26**, 12.
45 G. J. van Rooij, H. N. Akse, W. A. Bongers and M. C. M. van de Sanden, *Plasma Phys. Controlled Fusion*, 2018, **60**, 7.
46 G. X. Chen, F. Buck, I. Kistner, M. Widenmeyer, T. Schiestel, A. Schulz, M. Walker and A. Weidenkaff, *Chem. Eng. J.*, 2020, **392**, 7.
47 P. Fauchais and A. Vardelle, *IEEE Trans. Plasma Sci.*, 1997, **25**, 1258–1280.
48 L. F. Spencer and A. D. Gallimore, *Plasma Chem. Plasma Process.*, 2011, **31**, 79–89.
49 L. F. Spencer and A. D. Gallimore, *Plasma Sources Sci. Technol.*, 2013, **22**, 9.
50 Z. K. Li, T. Yang, S. J. Yuan, Y. X. Yin, E. J. Devid, Q. Huang, D. Auerbach and A. W. Kleyn, *J. Energy Chem.*, 2020, **45**, 128–134.
51 P. Fauchais and A. Vardelle, *Plasma Phys. Controlled Fusion*, 2000, **42**, B365–B383.
52 J. L. Blanchet, J. R. Parent and H. C. Lavallee, *Can. J. Chem. Eng.*, 1969, **47**, 160–165.
53 M. Gautier, V. Rohani and L. Fulcheri, *Int. J. Hydrogen Energy*, 2017, **42**, 28140–28156.
54 F. Fabry, C. Rehmet, V. Rohani and L. Fulcheri, *Waste Biomass Valorization*, 2013, **4**, 421–439.
55 A. Huczko and A. Szymanski, *Plasma Chem. Plasma Process.*, 1984, **4**, 59–72.
56 A. Huczko and A. Szymanski, *Zeitschrift Fur Physikalische Chemie-Leipzig*, 1982, **263**, 1210–1216.
57 V. Vermeiren and A. Bogaerts, *J. Phys. Chem. C*, 2020, **124**, 18401–18415.
58 J. Li, X. Q. Zhang, J. Shen, T. C. Ran, P. Chen and Y. X. Yin, *J. CO2 Util.*, 2017, **21**, 72–76.
59 T. Yang, J. Shen, T. C. Ran, J. Li, P. Chen and Y. X. Yin, *Plasma Sci. Technol.*, 2018, **20**, 9.
60 R. Aerts, R. Snoeckx and A. Bogaerts, *Plasma Process. Polym.*, 2014, **11**, 985–992.
61 A. H. Khoja, M. Tahir and N. A. S. Amin, Energy Convers, *Manag*, 2019, **183**, 529–560.

62 X. Tu and J. C. Whitehead, *Appl. Catal., B*, 2012, **125**, 439–448.
63 S. Ravasio and C. Cavallotti, *Chem. Eng. Sci.*, 2012, **84**, 580–590.
64 Q. Chen, W. Dai, X. M. Tao, H. Yu, X. Y. Dai and Y. X. Yin, *Plasma Sci. Technol.*, 2006, **8**, 181–184.
65 H. L. Long, S. Y. Shang, X. M. Tao, Y. P. Yin and X. Y. Dai, *Int. J. Hydrogen Energy*, 2008, **33**, 5510–5515.
66 X. M. Tao, F. W. Qi, Y. P. Yin and X. Y. Dai, *Int. J. Hydrogen Energy*, 2008, **33**, 1262–1265.
67 Y. Xu, Q. Wei, H. L. Long, X. Q. Zhang, S. Y. Shang, X. Y. Dai and Y. X. Yin, *Int. J. Hydrogen Energy*, 2013, **38**, 1384–1390.
68 X. Q. Zhang, C. H. Yang, Y. P. Zhang, Y. Xu, S. Y. Shang and Y. X. Yin, *Int. J. Hydrogen Energy*, 2015, **40**, 16115–16126.
69 P. Liu, X. S. Liu, J. Shen, Y. X. Yin, T. Yang, Q. Huang, D. Auerbach and A. W. Kleiyn, *Plasma Sci. Technol.*, 2019, **21**, 4.
70 J. M. Bermudez, E. Ruisanchez, A. Arenillas, A. H. Moreno and J. A. Menendez, Energy Convers, *Manag*, 2014, **78**, 559–564.
71 J. Hunt, A. Ferrari, A. Lita, M. Crosswhite, B. Ashley and A. E. Stiegman, *J. Phys. Chem. C*, 2013, **117**, 26871–26880.
72 W. Jin, Q. Huang, H. Xu and A. W. Kleyn, *Encyclopedia of Interfacial Chemistry: Surface Science and Electrochemistry*, 2017.
73 Q. Huang, D. Y. Zhang, D. P. Wang, K. Z. Liu and A. W. Kleyn, *J. Phys. D: Appl. Phys.*, 2017, **50**, 6.
74 D. Y. Zhang, Q. Huang, E. J. Devid, E. Schuler, N. R. Shiju, G. Rothenberg, G. van Rooij, R. L. Yang, K. Z. Liu and A. W. Kleyn, *J. Phys. Chem. C*, 2018, **122**, 19338–19347.
75 R. L. Yang, D. Y. Zhang, K. W. Zhu, H. L. Zhou, X. Q. Ye, A. W. Kleyn, Y. Hu and Q. Huang, *Acta Phys.-Chim. Sin.*, 2019, **35**, 292–298.
76 E. Devid, M. Ronda-Lloret, D. Zhang, D. Wang, C.-H. Liang, Q. Huang, G. Rothenberg, N. R. Shiju and A. Kleyn, *Chin. J. Chem. Phys.*, 2020, **33**, 243–251.
77 E. J. Devid, D. Zhang, D. Wang, M. Ronda-Lloret, Q. Huang, G. Rothenberg, N. R. Shiju and A. Kleyn, *Energy Technol.*, 2020, 1900886.
78 E. Devid and A. W. Kleyn, to be published.
79 V. J. Murray, P. Recio, A. Caracciolo, C. Miossec, N. Balucani, P. Casavecchia and T. K. Minton, *Carbon*, 2020, **167**, 388–402.